RSC Advances

PAPER

Cite this: *RSC Adv.*, 2020, **10**, 33071

Carbon fibers for treatment of cancer metastasis in bone

Takayuki Kamanaka,[a] Hisao Haniu,[ab] Manabu Tanaka,[a] Takashi Takizawa,[a] Kaoru Aoki,[ac] Masanori Okamoto,[a] Atsushi Sobajima,[a] Kazushige Yoshida,[a] Hirokazu Ideta,[a] Tetsuhiko Mimura,[a] Haruka Ishida,[b] Katsuya Ueda,[b] Takeshi Uemura,[bd] Jin Hee Kim,[e] Yoong Ahm Kim,[e] Hiroyuki Kato[a] and Naoto Saito *[bc]

When cancer metastasizes to bone, the resulting pain and functional disorders due to bone destruction adversely affect the patient's quality of life. We have developed a new cancer metastasis control system consisting of anticancer agents conjugated to carbon fibers (CFs), which are nonbiodegradable, carriers of a wide variety of molecules with extremely high affinity for bone. In the evaluation of cancer suppression effects on Walker 256 cancer cells, cisplatin (CDDP)-conjugated CFs (CF-CDDP) were found to be as effective in cancer suppression as CDDP. In the evaluation of the cancer suppression effects of local injection in the rat model of tibial cancer bone metastasis, similar cancer suppression was noted in the CF-CDDP group and CDDP group; however, blood Pt concentrations were significantly lower in the CF-CDDP group. Experiments with CDDP and CF-CDDP injected into bone actually destroyed by cancer metastases revealed the presence of significantly more newly formed bone tissue with the administration of CF-CDDP. Local administration of CF-CDDP is expected to become the first therapy to suppress cancer growth with low prevalence of adverse reactions, and to repair bone damaged by metastasis.

Received 27th May 2020
Accepted 28th August 2020

DOI: 10.1039/d0ra05992g

rsc.li/rsc-advances

Introduction

Cancer is one of the leading causes of death worldwide; the number of new patients is expected to reach 19 million in 2025.[1] More than two-thirds of patients with advanced breast cancer, prostate cancer, and lung cancer, in particular, will experience bone metastases.[2,3] When cancer metastasizes to bone, the patient's quality of life is largely affected mainly by severe pain and functional disorders due to bone destruction.[4] However, the molecular mechanism of pain in metastatic bone tumors remains incompletely elucidated, and clinically available non-steroidal anti-inflammatory drugs (NSAIDs) and opioid therapies are unable to control pain in about 45% of patients with metastatic bone tumors.[5] In addition, NSAIDs can cause gastrointestinal disorders and renal impairments, and opioids can cause drug resistance, constipation, and respiratory depression, making it difficult to control pain associated with their long-term use.[6,7] In spinal metastases of cancer, vertebral fractures and tumor infiltration in the spinal cord cause neurologic symptoms in the upper and lower extremities, and in serious cases, lead to muscle weakness and sensory disorders that are a major hindrance to daily activity.[8] Currently available therapeutic approaches for primary cancer loci consist of chemotherapy, radiotherapy, immunotherapy, and surgery.[9,10] Metastatic bone tumors are likely to develop in patients at the end stage of their illness where the primary locus of pain is uncontrollable even with such treatments. Although radiation is often used, adverse reactions are prevalent, making it extremely difficult to control the bone metastatic environment.[11,12]

We have developed a new system for treatment of cancer metastasized to bone comprising a conjugate of an anticancer agent and carbon fibers (CFs), designed for direct administration into lesions to kill cancer cells and promote repair of cancer-destroyed bone tissue. Traditionally, cancer treatment drug delivery systems (DDSs) and bone repair scaffolds have commonly been made of biodegradable materials; however, the environment of the bone metastatic site lacks orderliness so that the timing of sustained drug release and bone repair cannot be controlled satisfactorily with conventional materials.[11] CFs are only slightly degraded in living organisms, are likely to carry a wide variety of molecules with extremely high affinity for bone. Some studies have examined the anticancer

[a]*Department of Orthopaedic Surgery, Shinshu University School of Medicine, 3-1-1 Asahi, Matsumoto, Japan*
[b]*Institute for Biomedical Sciences, Interdisciplinary Cluster for Cutting Edge Research, Shinshu University, 3-1-1 Asahi, Matsumoto, Japan. E-mail: saitoko@shinshu-u.ac.jp*
[c]*Department of Applied Physical Therapy, Shinshu University School of Health Sciences, 3-1-1 Asahi, Matsumoto, Japan*
[d]*Division of Gene Research, Research Center for Supports to Advanced Science, Shinshu University, 3-1-1 Asahi, Matsumoto, Japan*
[e]*Faculty of Engineering, Chonnam National University, 77 Yongbong-ro, Buk-gu, Gwangju, Korea*

therapeutic effects of anticancer agent-bound carbon materials.[13–16] However, no study has attempted to examine the effects of a carbon material-based cancer treatment in the environment of a bone metastatic site. We have prepared a CF that is unlikely to enter small blood vessels, is likely to remain in the environment of a bone metastatic niche, and has the appropriate size for a bone regeneration scaffold. As such, CFs are surface-processed to make them suitable for conjugation with an anticancer agent (CDDP) (CF-CDDP). Having high bone affinity in addition, CFs are expected to serve as a scaffold for the repair of bone destroyed by cancer metastases.[17] In this paper, we evaluate the cancer suppression effect and systemic effect of CF-CDDP in the environment of a bone metastatic site, and the capacity of CFs to stimulate bone formation.

Results

CF-CDDP

CFs were prepared using an electrospinning method in which a high voltage is applied to polyacrylonitrile polymer in its molten state. We found that the average diameter of our nanofibers was *ca.* 400 nm and the average length was in the range of 20–100 μm. The real density of our sample was 1.7 mg mm^{-3} and the purity of carbon was above 99.1%. A large number of pores having a mean diameter of 2.79 nm were formed on the surface of the CFs. The CFs and CDDP (FUJIFILM Wako Pure Chemical Corporation, Osaka, Japan), along with a dispersant, were stirred and then centrifuged at 4000 rpm. The precipitated CF-CDDP was again dissolved in PBS and finally freeze-dried. The specific surface area was determined to be 3253 $mm^2\ g^{-1}$; the pore volume, to be 2.27 $cm^3\ g^{-1}$; and the CF-CDDP mass ratio, to be 3 : 10 (Fig. 1).

Sustained release capacity of CDDP

The amount of CDDP released from CF-CDDP was measured using an inductively coupled plasma (ICP) analysis system and a dialysis cassette (Slide-A-Lyzer, 20K MWCO, Filter size: 3 nm). About 50% of CDDP was released in 12 hours; and about 70%, in 24 hours. CDDP concentrations in the beaker tended to rise more slowly with CF-CDDP than with CDDP alone (Fig. 2).

Cell viability assay

The cell proliferation capacities of Walker 256 breast cancer cells in the presence of CFs, CDDP, and CF-CDDP were evaluated using an alamarBlue assay. On day 1, there was no significant difference in cell proliferation among the groups (day 1: 1.0000 ± 0.0668 in the control group, 0.8548 ± 0.0651 in the CF group, 0.8338 ± 0.0590 in the CDDP group, 0.8958 ± 0.0971 in the CF-CDDP group). On day 4, cell proliferation was suppressed in the CDDP group and CF-CDDP group, and similar cell proliferation was noted in the CF group compared with the control group (day 4: 1.0000 ± 0.0490 in the control group, 0.8299 ± 0.1052 in the CF group, 0.1169 ± 0.0459 in the CDDP group, 0.2709 ± 0.0564 in the CF-CDDP group). On day 8, the CF group showed cell proliferation similar to that found in the control group. In the CDDP group and CF-CDDP group, nearly all cancer cells died, with no significant difference noted (day 8: 1.0000 ± 0.1439 in the control group, 1.1519 ± 0.0413 in the CF group, 0.0211 ± 0.0073 in the CDDP group, 0.0322 ± 0.0160 in the CF-CDDP group). However, the number of viable

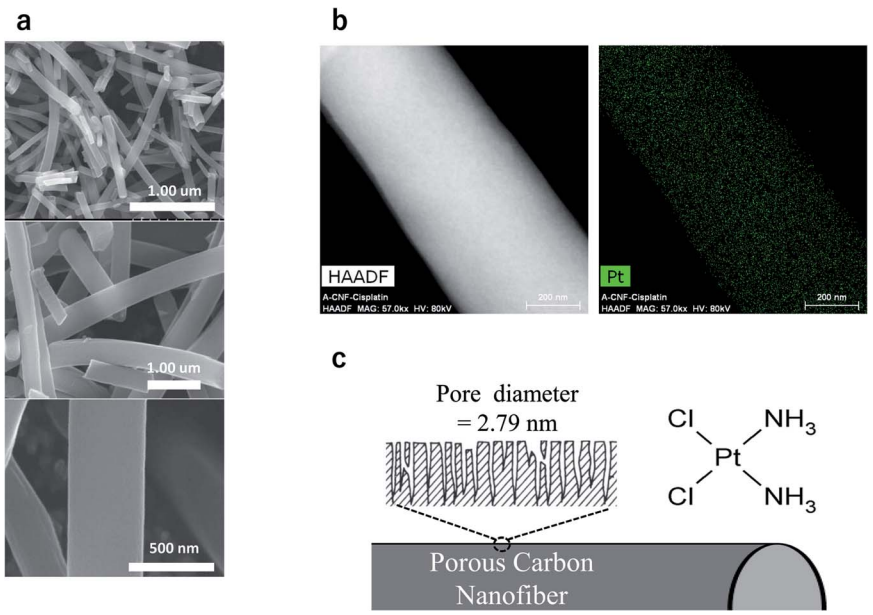

Fig. 1 Structure of CF-CDDP and Pt atom distribution. (a) CF-CDDP was structurally examined using a scanning electron microscope (SEM). CF-CDDP was found to have a fiber-entangled columnar structure with a diameter of 400 nm and a length of 20 to 100 μm. (b) Surface distribution of Pt atoms. Samples were examined by transmission electron microscope – energy dispersive X-ray spectroscopy (TEM-EDX). Pt atoms were evenly distributed on the CF surface. (c) The surface of CF-CDDP had a large number of pores having a mean diameter of 2.79 nm, with cisplatin found on the surface and inside.

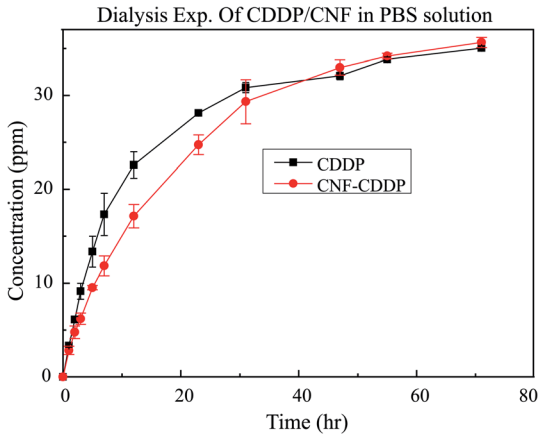

Fig. 2 Sustained release capacity of CDDP. The amount of CDDP released from CF-CDDP was measured over time up to 70 hours using an inductively coupled plasma (ICP) analysis system and a dialysis cassette (Slide-A-Lyzer, 20K MWCO, Filter size 3 nm) ($n = 3$). The dialysis cassette contained 6.0 mg of CDDP or 7.8 mg of CF-CDDP, and the beaker contained 100 mL of PBS. About 50% of CDDP was released in 12 hours; and about 70%, in 24 hours. Cisplatin concentrations in the beaker tended to rise more slowly with CF-CDDP than with CDDP alone.

cancer cells decreased more slowly in the CF-CDDP group than in the CDDP group (Fig. 3).

Cancer suppression effect

Walker 256 breast cancer cells were injected into the rat right tibia to develop a model of cancer bone metastasis. Two days later, CDDP at 10 mg kg^{-1} was injected into the same site (CDDP l.i. group). In addition, CF-CDDP with the same dose of CDDP was injected into the right tibial pulp chamber in the same manner (CF-CDDP l.i. group). The same dose of CDDP was injected *via* the right external jugular vein (CDDP i.v. group). Each group consisted of 5 animals ($n = 5$), and μCT imaging was performed at weeks 2 and 4. Four weeks later, the animals were sacrificed, and tissue sections were cut through the tibia at the median sagittal plane and evaluated. Cancer was not suppressed in the CDDP i.v. group. In both the CDDP l.i. group and the CF-CDDP l.i. group, on the other hand, cancer was suppressed (Fig. 4a). Tumor area in the median sagittal plane of the proximal tibia was minimized in the CF-CDDP l.i. group (Fig. 4b). Likewise, in the evaluation in the median sagittal plane of the tibia by μCT, bone destruction had progressed in the CDDP i.v. group, whereas none was noted in the CDDP l.i. group or CF-CDDP l.i. group (Fig. 4c).

Histological evaluation

Fig. 4a shows hematoxylin–eosin-stained tissue that has been sectioned through the median sagittal plane of a rat's tibia. In the control group and CDDP i.v. group, tumor tissue filled the pulp chamber. No evident difference was found between the two groups (tumor area: 11.3688 ± 2.3323 mm^2 in the control group, 9.4260 ± 3.0579 mm^2 in the CDDP i.v. group, $p = 0.1337$). Less tumor tissue and more fatty marrow were noted in the CDDP l.i. group than in the control group (tumor area: 11.3688 ± 2.3323 mm^2 in the control group, 1.0640 ± 1.2658 mm^2 in the CDDP l.i. group, $p = 0.0021$). In the CF-CDDP l.i. group, on the other hand, little tumor tissue or fatty marrow was noted, with much bone woven around the CFs (tumor area: 11.3688 ± 2.3323 mm^2

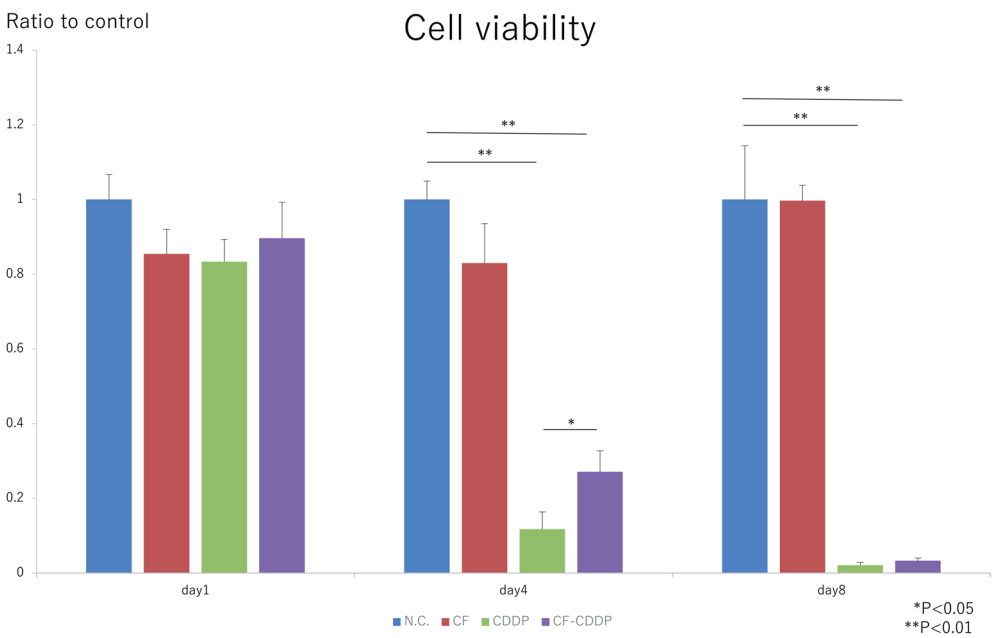

Fig. 3 Cell viability. The cell proliferation capacity of Walker 256 rat breast cancer cells was evaluated using an alamarBlue assay ($n = 5$). The CF group showed cancer cell proliferation similar to that found in the control group. The number of viable cancer cells decreased more slowly in the CF-CDDP group than in the CDDP group. Eventually, nearly all cancer cells died in both the CDDP group and the CF-CDDP group.

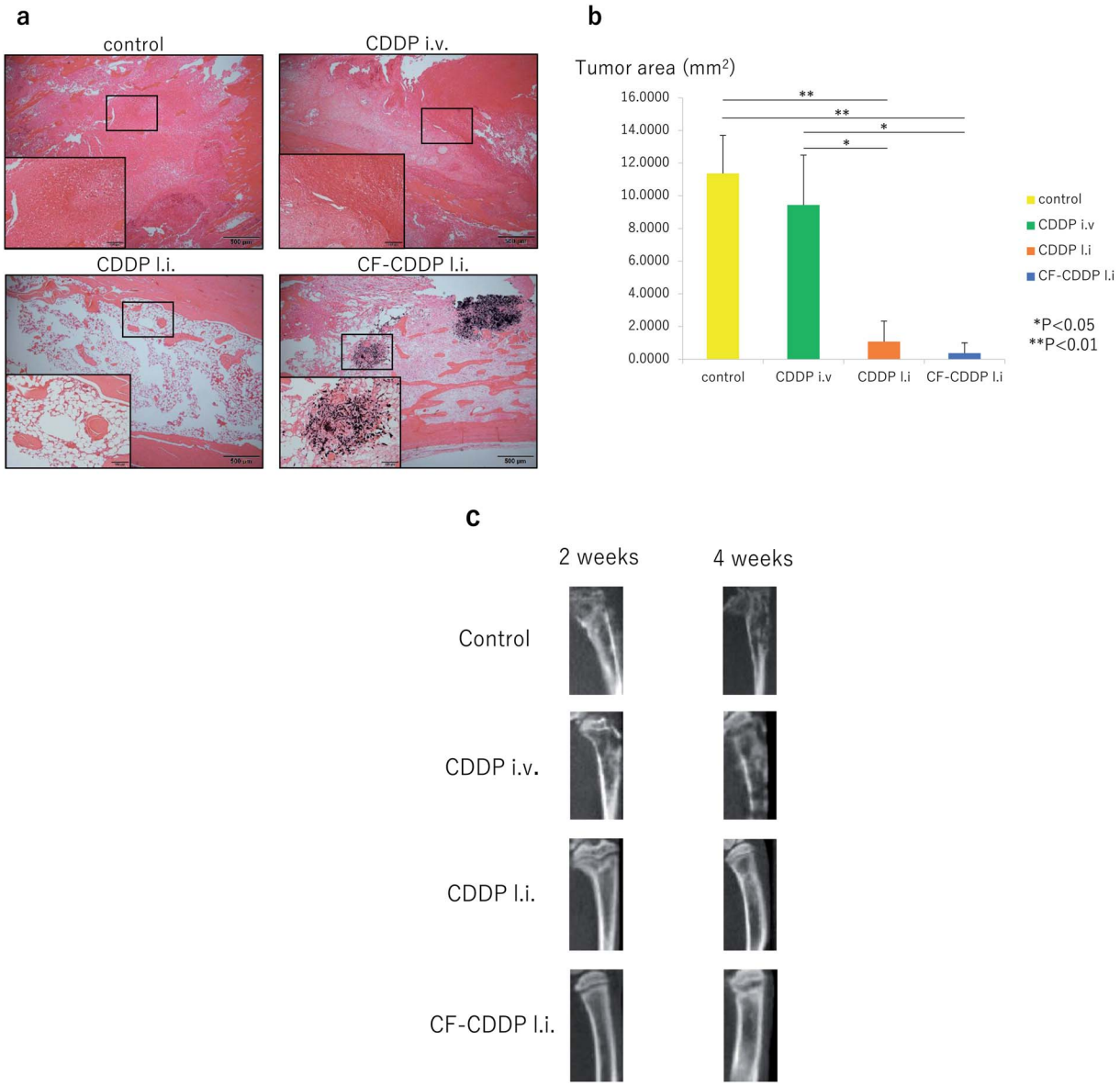

Fig. 4 Cancer suppression effect. (a) Tissue sections through the median sagittal plane of rat tibias with cancer metastasis, the rat model of cancer bone metastasis developed by injecting Walker 256 breast cancer cells into the rat tibia, were examined using a light microscope. Hematoxylin–eosin stained sections from the control group and CDDP i.v. group showed that tumor tissue occupied a large space in the pulp chamber. In the CDDP l.i. group, less tumor tissue and much fatty marrow was noted. In the CF-CDDP l.i. group, on the other hand, few tumor cells or little fatty marrow was noted, with much woven bone found around the CF. (b) The areas of the regions affected by cancer cells in the rat tibia were measured in the median sagittal plane ($n = 5$). Cancer was suppressed in the CDDP l.i. group and CF-CDDP l.i. group, but not in the CDDP i.v. group. (c) Cancer suppression was evaluated using median sagittal μCT images of the tibia. In the CDDP i.v. group, cancer was not suppressed, whereas in the CDDP l.i. group and CF-CDDP l.i. group, it was.

in the control group, 0.3802 ± 0.6147 mm^2 in the CF-CDDP l.i. group, $p = 0.0006$).

Blood concentration of anti-cancer agent

CDDP or CF-CDDP was locally injected into the right tibia of a rat model of cancer metastasis to the tibial bone, and blood was collected *via* the caudal vein 30 and 120 minutes later. In the group receiving CDDP injected *via* the right external jugular vein as well, blood was collected 30 and 120 minutes later ($n = 5$). At 30 minutes postdose, the blood platinum (Pt) concentration toughed at 1.0320 ± 0.4147 μg mL^{-1} in the CF-CDDP l.i. group, and was 1.6666 ± 0.6960 μg mL^{-1} in the CDDP l.i. group and 2.6380 ± 1.3187 μg mL^{-1} in the CDDP i.v. group. At 120 minutes postdose, the blood Pt concentration was 0.7040 ± 0.6160 μg mL^{-1} in the CF-CDDP l.i. group, 0.5040 ± 0.1280 μg mL^{-1} in the CDDP l.i. group, and 0.6700 ± 0.1513 μg mL^{-1} in the CDDP i.v. group. Compared with other groups, the CF-CDDP l.i. group had significantly lower blood Pt concentration at 30 minutes postdose, showing the least change over time. At 120 minutes postdose, the blood Pt concentration was similar among the groups (Fig. 5).

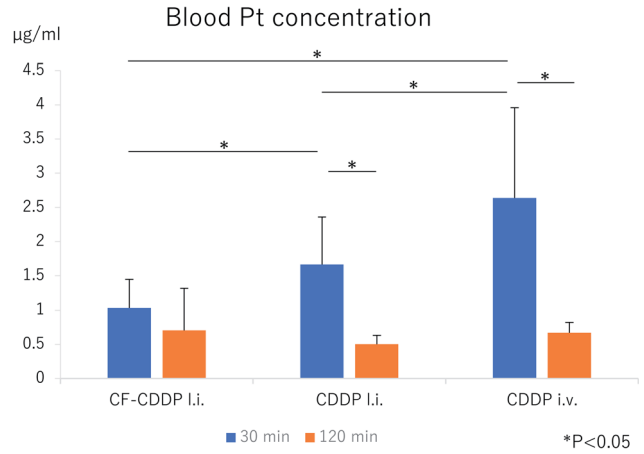

Fig. 5 Blood Pt concentrations. Two days after Walker 256 breast cancer cells were injected into the rat tibia, CF-CDDP or CDDP was locally injected and CDDP was injected intravenously ($n = 5$). At 30 and 120 minutes postdose, blood was collected *via* the rat caudal vein and assayed for Pt, a component of CDDP by atomic spectrophotometry. In the CF-CDDP l.i. group, the blood Pt concentration was significantly lower postdose, showing the least change over time. At 120 minutes postdose, the blood Pt concentration did not differ significantly among the groups.

Bone repair ability

In healthy female Wistar rats at 12 weeks of age, bone holes were made at the proximal ends of both tibias, using an 18-G needle. CFs, in a mixture with 50 μL of PBS, were injected into the right tibia at 3.0 mg kg^{-1}. Injected into the left tibia was 50 μL of PBS alone. Bone hole areas were evaluated on a horizontal sectional plane 5 mm distal to the rat knee joint plane, using μCT (Fig. 6a and b). Bone hole areas began to decrease in the CF group at week 6 (CF group: 0.99 ± 0.11 mm^2 at week 2, 0.71 ± 0.14 mm^2 at week 6, $p = 0.0423$), however, they were not significantly different from control group values (week 6: 0.85 ± 0.16 mm^2 in the control group, 0.71 ± 0.14 mm^2 in the CF group, $p = 0.1778$). At week 8, bone hole areas had decreased significantly in the CF group compared with the control group (week 8; 0.87 ± 0.08 mm^2 in the control group, 0.48 ± 0.16 mm^2 in the CF group, $p = 0.0164$).

Bone density

Results of μCT measurements showed that bone density up to 5 mm distal to the tibial knee joint plane was significantly higher at week 10 in the CF group than in the control group (week 0; 735.86 ± 40.49 mg cm^{-3} in the control group, 738.84 ± 33.87 mg cm^{-3} in the CF group: week 4; 848.20 ± 40.70 mg cm^{-3} in the control group, 833.10 ± 41.29 mg cm^{-3} in the CF group: week 10; 842.30 ± 60.46 mg cm^{-3} in the control group, 994.70 ± 12.41 mg cm^{-3} in the CF group, $p = 0.0309$) (Fig. 6c).

Bone neoplasticity in the bone metastatic environment

In the rat model of cancer bone metastasis, CDDP or CF-CDDP was locally injected into the right tibia, and CDDP was injected into the right external jugular vein. Four weeks later, tissue sections through the median sagittal plane of the tibia were subjected to Masson trichrome staining to stain woven bone light blue. Newly formed woven bone was evaluated in the control group, CDDP i.v. group, CDDP l.i. group, and CF-CDDP l.i. group. Woven bone area was significantly larger in the CF-CDDP l.i. group (0.0998 ± 0.1728 mm^2 in the control group, 0.0774 ± 0.1075 mm^2 in the CDDP i.v. group, 0.5344 ± 0.7233 mm^2 in the CDDP l.i. group, 3.5766 ± 0.6918 mm^2 in CF-CDDP l.i. group) (Fig. 7).

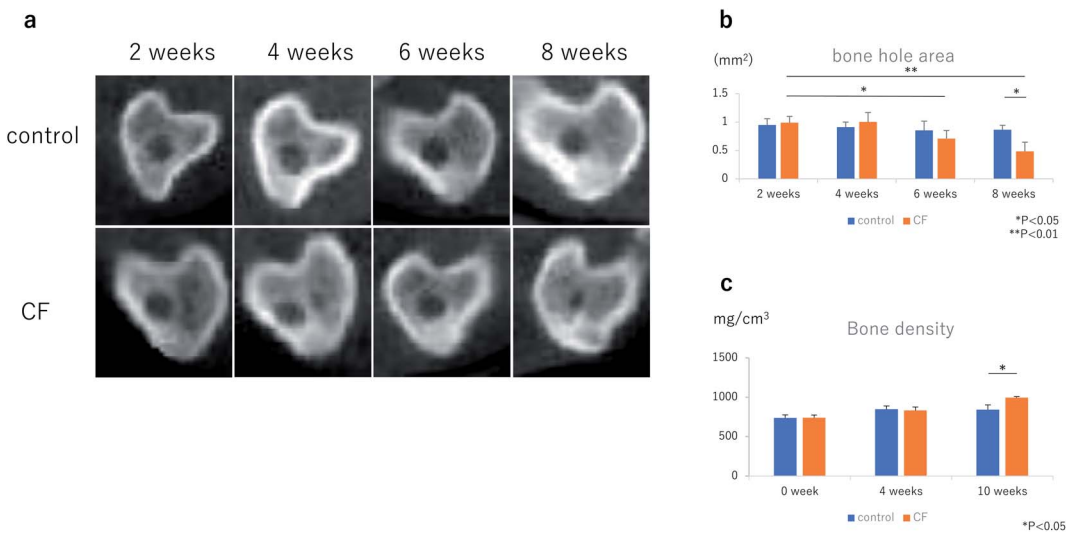

Fig. 6 Bone repair ability. (a) Bone repair ability was evaluated using μCT axial images 5 mm distal to the knee joint plane ($n = 5$). For the bone holes made in the rat tibia, bone hole area decreased earlier in the CF group than in the control group. (b) The areas of bone holes made in the rat tibia were measured at a level 5 mm distal to the knee joint ($n = 5$). Bone hole area decreased earlier in the CF group than in the control group. (c) Bone density at the rat proximal tibia was measured up to 5 mm distal to the knee joint ($n = 5$). At week 10, bone density was significantly higher in the CF group than in the control group.

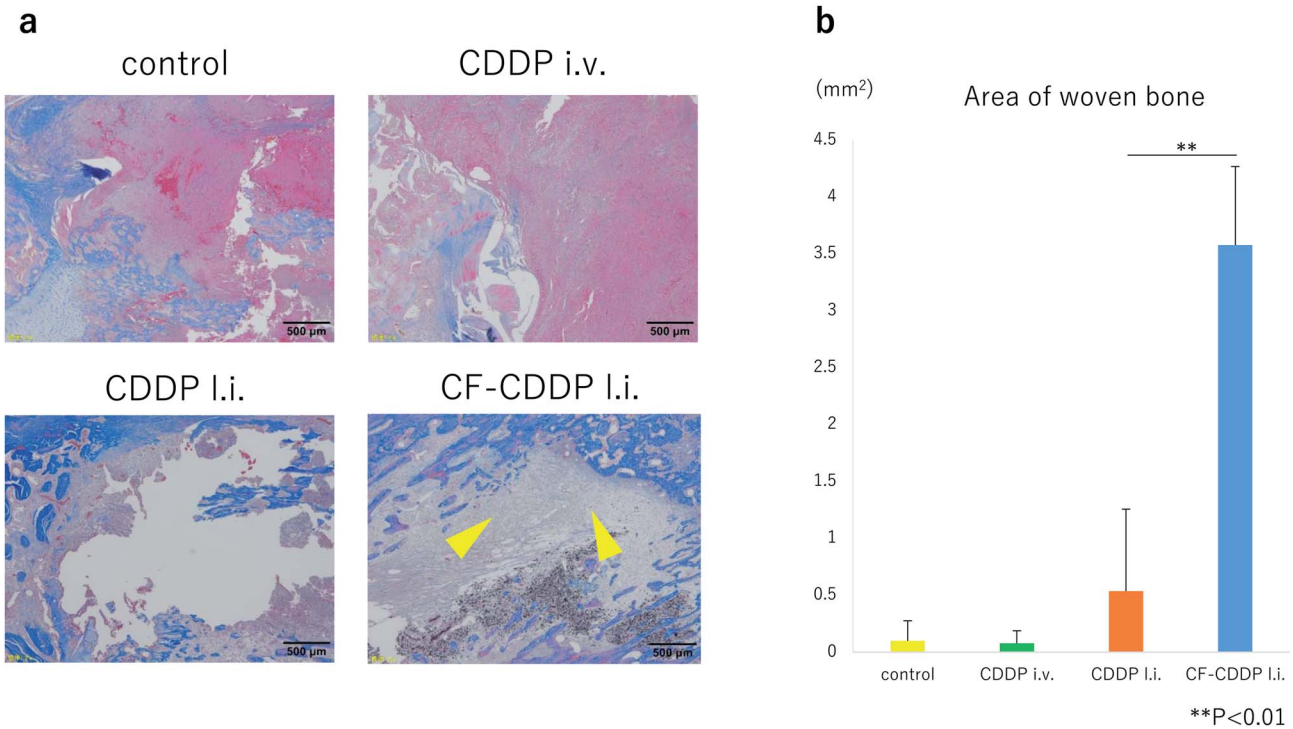

Fig. 7 Bone neoplasticity in the bone metastatic environment. (a) In the rat model of cancer bone metastasis (week 4), the tibia was dissected along the median sagittal plane, and Masson trichrome staining was performed to stain woven bone light blue. No evident woven bone was noted in the control group, CDDP i.v. group, or CDDP l.i. group, whereas in the CF-CDDP l.i. group, much woven bone was found around the CF (arrowhead). (b) The woven bone area at the median sagittal plane of the tibia ($n = 5$). Woven bone area was significantly larger in the CF-CDDP l.i. group.

Discussion

In recent years, a number of studies have been reported on the use of drug delivery systems (DDSs) of carbon material-conjugated anticancer agents in cancer treatment.[18–23] However, no available study has evaluated a carbon material-based DDS for treatment of bone metastasis. Carbon materials are useful in DDSs because their structural stability makes the surface easy to modify.[24] In addition, carbon materials are highly biocompatible, no stimulants of strong inflammatory responses in tissues around them.[25] In the present study, to sustain the release of an anticancer agent cisplatin (CPPD), we have succeeded in conjugating it with CFs of a size that makes them unlikely to enter small blood vessels, likely to remain in metastasis in bone, and likely to function as a bone regeneration scaffold. Sustained release is attributed to the fact that the drug is immobilized on fiber surfaces by a process (heating the CFs using an electrospinning method) that has no effect on fiber characteristics or drug bioactivity.[26] Fig. 2 shows the sustained release profile of the anticancer agent. The CFs released about 50% of the bound anticancer agent in 12 hours; and about 70%, in 24 hours. As such, the sustained release speed has been reported to vary depending on carbon material surface structure or ambient pH.[27–30] Although anticancer agent release can be slowed by regulating carbon nanofiber surface structure and ambient pH, this approach remains to be investigated in the future.

In the *in vitro* experiment, however, the suppression of cancer cell proliferation was delayed in the CF-CDDP group compared with the CDDP group. This is attributable to the fact that the amount of anticancer agent coming in contact with cancer cells increased slowly in the CF-CDDP group, as shown in the anti-cancer agent sustained-release test. Similarly, other results in the literature have shown the suppression of cancer cell proliferation by anti-cancer agent-conjugated carbon materials.[31]

In the *in vivo* experiments showed that cell proliferation was not suppressed in bone metastasis in the CDDP i.v. group. Many anticancer agents are of low solubility; when administered systemically, an extremely low proportion of anticancer agents reach metastatic lesions.[32] In the CDDP l.i. group and CF-CDDP l.i. group, on the other hand, cancer growth was evidently suppressed. This is attributable to the fact that the high anti-cancer agent concentration at the bone metastatic site was maintained by the direct sustained release of the anticancer agent into the site. In the present study, however, no significant difference was noted between the CDDP l.i. group and CF-CDDP l.i. group. In carbon-based DDSs, the release of anticancer agents is quicker in acidic environments such as around tumor cells, and slower at physiological pH.[33] In the present study, the anticancer agent release test was performed under neutral conditions for the following reason: although the tumor microenvironment is acidic, its pH varies depending on tumor nature and location. No specific pH levels are available for anticancer agent release tests, and many such tests reported in

the past were performed under neutral conditions.[34,35] While the absence of a significant difference in the present study remains unexplainable at present, it is necessary to elucidate the biochemical characteristics of the bone metastatic environment, and to optimize the use of CF-CDDP.

However, CFs were shown to be effective in maintaining blood concentrations of anticancer agents when used as DDSs. The blood concentration of anticancer agent was lowest 30 minutes postdose in the CF-CDDP l.i. group, and did not change substantially 120 minutes postdose. Hence, local injections of CF-CDDP into the bone metastatic site allowed the anticancer agent to remain localized and prevent rapid release and thereby elevation of the anticancer agent concentration in the blood.[36] Elevated blood levels of anticancer agents are known to lead to disorders of the heart, kidney, nervous system, and other organs.[37–39] Suppression of rapid elevations in blood levels of anticancer agent would reduce systemic adverse reactions to allow safer use of anticancer agents. The present study has proposed a useful system that is unlikely to cause adverse reactions even with the use of an anticancer agent in amounts sufficient to suppress tumors.

On the other hand, the bone formation capacity evaluation revealed bone sclerosis around the bone holes in the CF group at week 6, demonstrating reductions in bone hole cross-sectional area. At week 8, a significant difference was noted compared with the control group. Bone density at week 10 was significantly higher in the CF group than in the control group. Hence, early bone repair can be expected for bone defects with CF serving as a scaffold, at weeks 8 to 10. Furthermore, in experiments with CDDP and CF-CDDP injected into bone actually destroyed by cancer metastases, Masson trichrome staining, which stains woven bone light blue, revealed the presence of significantly more woven bone and newly formed bone tissue with the administration of CF-CDDP. Hence, CFs, serving as a scaffold for newly formed bone, were shown to promote bone repair even in cancer metastasis bone. CF-CDDP represents the first system to be capable of both suppressing cancer growth in the bone metastatic environment and repairing destroyed bone. We previously reported that carbon nanofibers caused very weak but observable inflammatory responses just after implantation *in vivo*; however, the inflammatory responses resolved quickly and did not occur again during the long period that followed.[17] In the present study, no inflammatory cells were found in tibial tissue sections collected 4 weeks after administration of CF-CDDP. For these reasons, we conjectured that inflammatory responses did not have a major influence on the efficacy of the anticancer agent CDDP or bone repair.

In the present study, the sustained release capacity and cancer suppression effect of the anticancer agent-CF conjugate, postdose blood levels of anticancer agent, and bone formation capacity were evaluated. The conjugate was shown to be unlikely to release the anticancer agent into the blood, thus reducing adverse reactions, even when the anticancer agent is used at doses sufficient to suppress cancer in the bone metastatic environment. Furthermore, CFs were shown to stay in bone destroyed by cancer metastases, and to serve as a bone repair scaffold. Having the binary effects of cancer suppression with decreased adverse reactions and repair of destroyed bone, this new cancer metastasis bone treatment system is expected to improve the prognosis for an ever-increasing number of cancer patients with bone metastases and their quality of life.

Experimental methods

Carbon fiber (CF)

The electrospinning dope was prepared by dissolving 15 wt% of the PAN polymer (reagent grade, 98%, Sigma-Aldrich, USA) in *N*,*N*′-dimethylformamide (DMF, extra pure grade, Duksan Pure Chemicals Co., Ltd, Korea). The organic nanofiber web was obtained using the electrospinning apparatus (NT-ESS_300, NTSEE Co., Korea) under the following conditions: tip-to-collector distance, 18 cm; applied voltage, 25 kV; feeding rate, 4 mL h^{-1}. The organic nanofiber web was air stabilized at 280 °C for 1 h. Then, the air-stabilized nanofiber web was chemically activated at 800 °C in order to improve the porosity on the carbon nanofiber surface. The average diameter of our nanofibers was *ca.* 400 nm and the average length was in the range of 20–100 μm. The real density of our sample was 1.7 mg mm^{-3} and the purity of carbon was above 99.1%.

Cisplatin (CDDP)

The CDDP used in the present study was a pharmacological-grade product of FUJIFILM Wako Pure Chemical Corporation (Osaka, Japan), 033–20 091, Lot WDF6849.

CF-CDDP

CF was obtained using an electrospinning method in which a high voltage is applied to polyacrylonitrile polymer in its molten state. CF, along with KOH, was heated at 800–900 °C to increase its surface area. A large number of pores having a mean diameter of 2.79 nm were formed on the CF surface. CF or CDDP, along with the dispersant DMF, was stirred and then centrifuged at 4000 rpm. The precipitated CF-CDDP was again dissolved in PBS and finally freeze-dried (Fig. 1). The specific surface area was determined to be 3253 mm^2 g^{-1} and the pore volume, to be 2.27 cm^3 g^{-1}. The CF-CDDP mass ratio was determined to be 3 : 10. CF-CDDP consisting of 0.46 mg of CF and 1.54 mg of CDDP per well was used in the *in vitro* experiment, whereas CF-CDDP consisting of 0.6 mg of CF and 2.0 mg of CDDP was used in the *in vivo* (tibial injection) experiment. CDDP is considered to be physically bound in the multiple pores on the CF surface when blended with a dispersant and freeze-dried.

Cell viability assay

Walker 256 rat breast cancer cells (Riken Cell Bank, Tokyo, Japan. RBRC-RCB2909) were seeded to a 24-well plate at a density of 2×10^4 cells per well and allowed to adhere to the plate in a medium (RPMI 1640) over 24 hours. Thereafter, a Millicell insert (Merck Millipore Ltd, Germany) with CF, CDDP, or CF-CDDP set thereon was placed in each well ($n = 5$). CF was used at a concentration of 3.75 μg/200 μL per well; CDDP, at 6.25 μg/200 μL per well; and CF-CDDP, at 10.0 μg/200

μL per well. The Millicell insert is a cell culture insert having a diameter of 12 mm and a membrane on the bottom that is penetrable by CDDP but not by CF. The proliferation capacity of Walker 256 cells was evaluated using an alamarBlue assay 1, 4, and 8 days after placement of the Millicell. Fluorescence intensity values were compared with those from the control group on the various evaluation days. To discard the CDDP remaining in the medium, RPMI 1640 medium was replaced with a fresh supply on every measuring day. Thereafter, the Millicell in use was replaced.

In vitro drug release

The amount of CDDP released from CF-CDDP was measured over time up to 70 hours using an inductively coupled plasma (ICP) analysis system and a dialysis cassette (Slide-A-Lyzer, 20K MWCO, Filter size: 3 nm) ($n = 3$). The dialysis cassette contained 6.0 mg of CDDP or 7.8 mg of CF-CDDP, and the beaker contained 100 mL of PBS.

Rat model of cancer bone metastasis

Female Wistar rats at 12 weeks of age (SLC, Shizuoka, Japan) were sedated by inhalation anesthesia with 3% isoflurane (Abbott Japan, Tokyo, Japan). Bone holes were made at the proximal ends of the right tibia using an 18-G needle, Walker 256 breast cancer cells were injected with 1×105 cells, and the bone holes were closed with bone wax using a microsyringe and 27-G needle. Two weeks later, μCT revealed a bone metastasis in the tibial pulp chamber (Fig. 4c). Four weeks later, the rats were euthanized by high-dose inhalation of isoflurane. In the tissue section through the tibial median sagittal plane (H.E. staining), cancer cell proliferation and occupancy in the pulp chamber were noted (Fig. 4a).

All animal procedures were performed in accordance with the Guidelines for Care and Use of Laboratory Animals of Shinshu University and approved by the Animal Ethics Committee of Shinshu University.

Local injection of CDDP and CF-CDDP into the tibia

Walker 256 breast cancer cells were injected into the proximal end of the right tibia. Two days later, CDDP at 10 mg kg^{-1} was injected into the same site. In addition, CF-CDDP with the same absolute dose of CDDP was injected into the right tibial pulp chamber in the same manner ($n = 5$). The bone holes were closed with bone wax to prevent the drug from leaking. Two and four weeks later, tibial bone metastases in the pulp chamber were examined under operating conditions of 80 kV, 80 μA, and 18-second exposure time, using the μCT (R_mCT, manufactured by Rigaku Corporation, Tokyo, Japan). Four weeks later, tissue sections were cut from the right tibia through the median sagittal plane and stained with hematoxylin–eosin (H.E.). Tumor tissues were present mainly in the proximal tibia, and tumor areas were measured up to 5 mm distal to the knee joint plane using ImageJ software.[40] To evaluate newly formed bone, Masson trichrome staining was performed. The area of woven bone was measured using the ImageJ software in the same manner.

Intravenous injection of CDDP

Walker 256 breast cancer cells were injected into the rat tibia, and CDDP was injected *via* the external jugular vein 2 days later. About a 1 cm incision was made in the skin on the right side of the neck in each rat sedated by isoflurane inhalation anesthesia, and CDDP at 10 mg kg^{-1} was injected *via* the right external jugular vein using a 27-G needle ($n = 5$). Two and four weeks later, tibial bone metastases in the pulp chamber were examined using μCT. Four weeks later, the rats were euthanized by high-dose inhalation of isoflurane, and tissue sections were cut through the right tibia at the median sagittal plane and stained with H.E. Tumor areas were measured up to 5 mm distal to the knee joint plane using the ImageJ software.

Blood concentration of anti-cancer agent

CDDP or CF-CDDP was locally injected into the right tibia of a rat model of tibial bone cancer metastasis, and blood was collected *via* the caudal vein 30 and 120 minutes later. In the group receiving CDDP injected *via* the right external jugular vein as well, blood was collected 30 and 120 minutes later ($n = 5$). As a blood sample parameter, concentration of platinum (Pt), a component of CDDP, was measured by atomic spectrophotometry (SRL, Nagano, Japan).

Bone repair ability

In healthy female Wistar rats at 12 weeks of age, bone holes were made at the proximal ends of both tibias, using an 18-G needle. CF mixed with PBS was injected into the right tibia at a dose of 3.0 mg kg^{-1} in a total volume of 50 μL. PBS alone, 50 μL, was injected into the left tibia. The tibial bone holes were closed with bone wax. Cross-sectional views of the bone holes were evaluated using μCT ($n = 5$) 2, 4, 6, and 8 weeks later. The cross-sectional area of each bone hole was measured on a horizontal section 5 mm distal to the knee joint plane, using ImageJ software. In the same model, rat tibial bone density up to 5 mm distal to the knee joint was measured using μCT at weeks 0, 4, and 10 ($n = 5$).

Statistical analysis

Data are expressed as the mean and standard deviation. Statistical analyses were carried out using the statistical package R, version 3.5.2 (available at: https://www.r-project.org). The level of significance was set at $p < 0.05$.

Author contributions

N. S. conceived the original concept. N. S. conceptualized the study. T. K and N. S. designed, performed, oversaw, interpreted, and generated data and figures. T. K. and A. S performed and analyzed *in vivo* experiments and data. H. H. and T. U advised on study design and statistical analysis. H. H. supervised the study. T. K. and N. S. wrote the manuscript. All authors read and edited the manuscript.

Conflicts of interest

The authors declare no conflict of interest.

Acknowledgements

We would like to extend our gratitude to Toru Hiraga at the Department of Histology and Cell Biology of Matsumoto Dental University. We would like to thank the staff at the Division of Instrumental Analysis and Division of Animal Research at the Research Center for Supports to Advanced Science of Shinshu University for their assistance. This research was supported by the Grant-in-Aid for Scientific Research No. 17H0158400 from Japan's Ministry of Health, Labor and Welfare.

References

1 B. W. Stewart and C. P. Wild, *International Agency for Research on Cancer, World Cancer Report 2014*. Lyon, France, 2014.
2 B. T. Li, M. H. Wong and N. Pavlakis, *J. Clin. Med.*, 2014, **3**, 1–24.
3 A. Turabi and A. R. Plunkett, *J. Surg. Oncol.*, 2012, **105**, 494–501.
4 C. Ferrer Albiach, F. Villegas Estévez, M. D. López Alarcón, M. de Madariaga, A. Carregal, J. Arranz, J. M. Trinidad Martín-Arroyo, A. J. Jiménez López and A. Sanz Yagüe, *J. Pain Res.*, 2019, **12**, 2125–2135.
5 T. Meuser, C. Pietruck, L. Radbruch, P. Stute, K. A. Lehmann and S. Grond, *Pain*, Lippincott Williams & Wilkins, 2001, vol. 93, pp. 247–257.
6 C. Pacharinsak and A. Beitz, *Comp. Med.*, 2008, **58**, 220–233.
7 A. P. Borda, F. Charnay-Sonnek, V. Fonteyne and E. G. Papaioannou, *Guidelines on Pain Management and Palliative Care*, European Association of Urology, 2013.
8 I. M. Adjei, M. N. Temples, S. B. Brown and B. Sharma, *Pharmaceutics*, 2018, **10**, 205.
9 M. Arruebo, N. Vilaboa, B. Sáez-Gutierrez, J. Lambea, A. Tres, M. Valladares and A. González-Fernández, *Cancers*, 2011, **3**, 3279–3330.
10 E. Lee, J. Koo and T. Berger, *Int. J. Dermatol.*, 2005, **44**, 355–360.
11 S. Y. Madani, N. Naderi, O. Dissanayake, A. Tan and A. M. Seifalian, *Int. J. Nanomed.*, 2011, **6**, 2963–2979.
12 A. A. Butala, S. S. Lo and J. A. Jones, *Ann. Palliat. Med.*, 2019, **8**, 337–351.
13 Z. Liu, A. C. Fan, K. Rakhra, S. Sherlock, A. Goodwin, X. Chen, Q. Yang, D. W. Felsher and H. Dai, *Angew. Chem. Int. Ed.*, 2009, **48**, 7668–7672.
14 F. Wang, Q. Sun, B. Feng, Z. Xu, J. Zhang, J. Xu, L. Lu, H. Yu, M. Wang, Y. Li and W. Zhang, *Adv. Healthc. Mater.*, 2016, **5**, 2227–2236.
15 X. Zhang, Y. Wang, W. Liu, X. Liang, B. Si, E. Liu, X. Hu and J. Fan, *Mater. Lett.*, 2017, **209**, 360–364.
16 Y. Huang, P. Xie, S. T. Yang, X. Zhang, G. Zeng, Q. Xin and X. H. Tang, *Mater. Sci. Eng., C*, 2018, **92**, 416–423.
17 K. Aoki, Y. Usui, N. Narita, N. Ogiwara, N. Iashigaki, K. Nakamura, H. Kato, K. Sano, N. Ogiwara, K. Kametani, C. Kim, S. Taruta, Y. A. Kim, M. Endo and N. Saito, *Small*, 2009, **5**, 1540–1546.
18 A. Guven, G. J. Villares, S. G. Hilsenbeck, A. Lewis, J. D. Landua, L. E. Dobrolecki, L. J. Wilson and M. T. Lewis, *Acta Biomater.*, 2017, **58**, 466–478.
19 Y. Ren and G. Pastorin, *Adv. Mater.*, 2008, **20**, 2031–2036.
20 A. Guven, I. A. Rusakova, M. T. Lewis and L. J. Wilson, *Biomaterials*, 2012, **33**, 1455–1461.
21 J. Li, A. Pant, C. F. Chin, W. H. Ang, C. Ménard-Moyon, T. R. Nayak, D. Gibson, S. Ramaprabhu, T. Panczyk, A. Bianco and G. Pastorin, *J. Nanomed. Nanotechnol.*, 2014, **10**, 1465–1475.
22 A. Mejri, D. Vardanega, B. Tangour, T. Gharbi and F. Picaud, *J. Phys. Chem. B*, 2015, **119**, 604–611.
23 T. A. Hilder and J. M. Hill, *Small*, 2009, **5**, 300–308.
24 F. Badrzadeh, M. Rahmati-Yamchi, K. Badrzadeh, A. Valizadeh, N. Zarghami, S. M. Farkhani and A. Akbarzadeh, *Artif. Cells, Nanomed., Biotechnol.*, 2016, **44**, 618–634.
25 A. Yokoyama, Y. Sato, Y. Nodasaka, S. Yamamoto, T. Kawasaki, M. Shindoh, T. Kohgo, T. Akasaka, M. Uo, F. Watari and K. Tohji, *Nano Lett.*, 2005, **5**, 157–161.
26 S. Chen, S. K. Boda, S. K. Batra, X. Li and J. Xie, *Adv. Healthc. Mater.*, 2018, **7**, 1701024.
27 N. Suo, M. Wang, Y. Jin, J. Ding, X. Gao, X. Sun, H. Zhang, M. Cui, J. Zheng, N. Li, X. Jin and S. Jiang, *Int. J. Nanomed.*, 2019, **14**, 1241–1254.
28 L. Saeednia, L. Yao, K. Cluff and R. Asmatulu, *ACS omega*, 2019, **4**, 4040–4048.
29 J. Yang, H. Su, W. Sun, J. Cai, S. Liu, Y. Chai and C. Zhang, *Theranostics*, 2018, **8**, 1966–1984.
30 Q. Zhao, Y. Lin, N. Han, X. Li, H. Geng, X. Wang, Y. Cui and S. Wang, *Drug Delivery*, 2017, **24**(supp. 1), 94–107.
31 J. Li, S. Q. Yap, S. L. Yoong, T. R. Nayak, G. W. Chandra, W. H. Ang, T. Panczyk, S. Ramaprabhu, S. K. Vashist, F. S. Sheu, A. Tan and G. Pastorin, *Carbon*, 2019, **50**, 1625–1634.
32 H. Hyun, Y. B. Yoo, S. Y. Kim, H. S. Ko, H. J. Chun and D. H. Yang, *Int. J. Mol. Sci.*, 2019, **20**, 4671.
33 Q. Guo, X. T. Shen, Y. Y. Li and S. Q. Xu, *J. Huazhong Univ. Sci. Technol., Med. Sci.*, 2017, **37**, 635–641.
34 L. Pang, Y. Zhu, J. Qin, W. Zhao and J. Wang, *Drug Delivery*, 2018, **25**, 1922–1931.
35 D. Ailincai, L. T. Mititelu and L. Marin, *Drug Delivery*, 2018, **25**, 1080–1090.
36 A. P. Singh, A. Biswas, A. Shukla and P. Maiti, *Signal Transduction Targeted Ther.*, 2019, **30**, 33.
37 M. Volkova and R. Russell, *Curr. Cardiol. Rev.*, 2011, **7**, 214–220.
38 M. H. Hanigan and P. Devarajan, *Cancer Ther.*, 2003, **1**, 47–61.
39 R. Velasco, *J Bruna. Toxics*, 2015, **3**, 152–169.
40 W. S. Rasband, *ImageJ*, U. S. National Institutes of Health, Bethesda, Maryland, USA, 1997–2018, https://imagej.nih.gov/ij/.